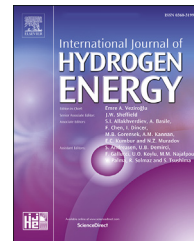




ELSEVIER

Available online at [www.sciencedirect.com](http://www.sciencedirect.com)

ScienceDirect

journal homepage: [www.elsevier.com/locate/he](http://www.elsevier.com/locate/he)

# Enthalpy analysis of Ce–Mg–Ni–H formation based on extended miedema theory: Investigation of selected $\text{Ce}_2\text{MgNi}_2\text{--H}_2$

Zhuocheng Liu <sup>a,b,\*</sup>, Yiming Li <sup>a,\*\*</sup>, Fei Ruan <sup>a</sup>, Guofang Zhang <sup>a</sup>,  
Ming Zhao <sup>a</sup>, Zhongxin Liu <sup>a</sup>, Jieyu Zhang <sup>b</sup>

<sup>a</sup> Key Laboratory of Integrated Exploitation of Bayan Obo Multi-Metal Resources, Inner Mongolia University of Science and Technology, Baotou, 014010, China

<sup>b</sup> Shanghai Key Laboratory of Modern Metallurgy & Materials Processing, Shanghai University, Shanghai, 200072, China

## HIGHLIGHTS

- Formation enthalpies of hydrogen-containing quaternary are calculated by extended Miedema's model.
- Estimated maximum hydrogen content is found to correspond to the most negative enthalpy.
- Maximum hydrogen capacity of  $\text{Ce}_2\text{MgNi}_2$  alloy reaches 1.57 wt. %  $\text{H}_2$ , this is consistent with theoretical H-storage 1.64 wt. %  $\text{H}_2$ .
- Hydride formation enthalpy of  $\text{Ce}_2\text{MgNi}_2$  alloy is  $-63.7 \text{ kJ/mol}$ . It keeps with  $-59.1 \text{ kJ/mol}$   $\text{H}_2$  obtained by Van't Hoff equation.

## ARTICLE INFO

### Article history:

Received 16 June 2020

Received in revised form

12 October 2020

Accepted 23 October 2020

Available online 16 November 2020

## ABSTRACT

In this paper, an extended Miedema's model is constructed to illustrate its applicability to estimating the solid-solution enthalpies of Ce–Mg–Ni–H hydrides, adopting the range of an optimized stoichiometry alloy in the contour map of solid-solution state enthalpy.  $\text{Ce}_2\text{MgNi}_2$  alloy is designed to investigate its hydrogen storage properties, and its main phase is confirmed with X-ray diffraction characterizations. The alloy shows a good activation ability and the pressure component temperature plateau is extremely flat. The formation enthalpy of  $\text{Ce}_2\text{MgNi}_2\text{--H}_2$  is calculated with the extended Miedema theory, with the least enthalpy value of  $-59.1 \text{ kJ/mol}$  for the corresponding hydrogen content of 1.64 wt %. Both experimental and theoretical data of the hydrogen-containing alloy confirm that the thermodynamic enthalpy of the quaternary  $\text{Ce}_2\text{MgNi}_2\text{--H}_2$  is consistent with that of the experimental results. When calculating the formation enthalpy of hydrogen and metal, the enthalpy of the elastic contribution between metal and hydrogen was considered, generally improving the versatility and accuracy of the calculation. Moreover, the extended Miedema's model is used to predict the hydrogen storage performance.

© 2020 Hydrogen Energy Publications LLC. Published by Elsevier Ltd. All rights reserved.

### Keywords:

Hydrogen storage alloys

Thermodynamic modeling

Miedema theory

Gas–solid reactions

\* Corresponding author. Key Laboratory of Integrated Exploitation of Bayan Obo Multi-Metal Resources, Inner Mongolia University of Science and Technology, 014010, Baotou, China.

\*\* Corresponding author.

E-mail addresses: [liuzhuo567@eyou.com](mailto:liuzhuo567@eyou.com) (Z. Liu), [liyiming79@sina.com](mailto:liyiming79@sina.com) (Y. Li).

<https://doi.org/10.1016/j.ijhydene.2020.10.195>

0360-3199/© 2020 Hydrogen Energy Publications LLC. Published by Elsevier Ltd. All rights reserved.

## Introduction

In recent years, hydrogen storage materials have drawn tremendous attentions due to their potential applications in the development of hydrogen energy economy. Among the various hydrogen storage materials, the researches on intermetallic compounds for hydrogen storage have received intense interests because of their excellent material structures and hydrogen storage properties. They have found wide application, such as hydrogen adsorption in metal-organic frameworks (MOFs) [1], cathode materials for batteries [2], high-entropy alloys [3], metal hydride and its alloy hydride [4,5], metal-glass [6]. In these applications, the thermodynamic properties of a hydrogen storage material are significant, which govern the hydrogen storage capacity and operating temperature. A number of isotherm models have been used to discuss and calculate the absorption and desorption thermodynamic data of the hydrogen storage compounds. Miedema's model is the one of these models. It has been widely applied in many areas, such as calculating the standard formation enthalpy of intermetallic compounds and liquid-phase alloys [7,8]. As well as predicting and assisting in the calculation of phase diagrams and thermodynamic properties [9], determining crystal stability of phase in multicomponent alloy systems [10]. And then theoretically scrutinizing the amorphous forming composition range (AFCR) theoretically and glass forming ability (GFA) [11], and investigating the mixing interaction on interface of solid-liquid system [12].

Moreover, with Miedema's models, it is relatively simple to predict the formation enthalpy or Gibbs energy of amorphous and crystalline intermetallic compounds [13,14]. This advantages is hard to achieve with other calculation methods, such as current first-principles calculations and atomistic simulation techniques. In addition, they are not economical and time-consuming, unfavorable predicting thermodynamic of multicomponent alloy. Liu et al. [6,15] employed Miedema's model and Alonso's method in thermodynamic calculations. It is revealed that the amorphous phase is favored in the large composition region in the Mg–Ni–Y system. This can be thought of as glass formation compositions first predicted by thermodynamic calculations based on the extended Miedema's model. As for the single phase high-entropy alloys (SPHEAs), King et al. [3] established that compare with the density functional theory (DFT), Miedema methodology is useful over a wider range of alloy compositions with far more permutations-by orders of magnitude. Moreover, the Miedema methodology tends to predict precipitation temperatures and the tendency of precipitation of SPHEAs. This approach is used to obtain and analyze the thermodynamic properties of the Ti–Nb–Ta–Mn system consistent with the experimental and thermodynamic results by Aguilaret al. [16]. Jacob et al. and Sreekumar et al. [17,18] calculated the enthalpy and Gibbs energy of the Gd–Rh–O, Al–Mg–O ternary alloy system, respectively, confirming that phase relations in the system ternary could be computed as a temperature function at constant oxygen partial pressures. Also calculated were the enthalpies of the binary and multivariate systems for non-metallic C, P and N [19–21], with the results matched with that of the experiment data. Accordingly, current efforts

are focused on finding the calculated formation enthalpy suitable for metal hydrides purposes.

Matysik [22] summarized the application of Pettifor stability structure maps to  $MH_x$  binary metal (M) hydrides in accordance with their hydrogenation properties. A comparison was also conducted on the enthalpy values obtained from experiments or calculations based on the Miedema, Born–Haber and Energetic models. The semi-empirical models showed a nearly satisfactory estimation of the binary hydride stability. The calculations of thermodynamic enthalpy for metals with hydrogen have been reported before [7], but they are limited to the binary or early Miedema's models. Hence, the most serious problems are the confined practicability and the wide off-margins of the calculation errors.

Ce–Mg–Ni alloys are of considerable interest for their excellent hydrogen storage properties [23–25]. There are several potential candidates for hydrogen storage in the Mg-rich corner of Ce–Mg–Ni ternary systems, such as  $Mg_{90}(Ce, Y)_{10-x}Ni_x$ , Mg–10Ni–2Mm (Mm is misch-metals), and Mg–Ce/Ni [26–28]. Quite a few researches have investigated the constituent binary systems of Ce–Mg–Ni using experimental and thermodynamic calculation methods. Some ternary phases have been reported in Ce–Mg–Ni ternary system, such as  $CeMgNi_9$  [29,30],  $CeMgNi_4$  [31,32],  $CeMgNi$  [33],  $Ce_2MgNi_2$  [31,34] and  $Ce_{23}Mg_4Ni_7$  [35]. However, there are few studies on the hydrogen storage properties of these compounds.

Our design is particularly critical for Ce–Mg–Ni–H alloy system as the foundation. The thermodynamic enthalpies are estimated by the extended Miedema model and compared with previously available experimental data and evaluations of the hydrogen storage performance, including the thermodynamic of hydrogenation properties executed on the results. In this study,  $Ce_2MgNi_2$  alloy is selected to investigate its activation performance and thermodynamic properties. According to our early estimation, the ternary phase of  $Ce_2MgNi_2$  is the most easily formed of all visible ternary phases. With this, it is verified that the enthalpies of ternary hydrides Ce–Mg–Ni–H coincided with that of the experimental data trends.

## Thermodynamic calculations

In order to predict the targeted thermodynamic enthalpy in a quaternary Ce–Mg–Ni–H system containing hydrogen. The formation enthalpies of the ternary and quaternary system are obtained by three pseudo-binary interpolations and four ternary interpolations respectively, as shown schematically in Fig. 1.

For the calculation and deduction process of ternary enthalpy of formation, our research group has made a detailed explanation in the literature is made [27]. Here, according to the derivation process of ternary, the formation enthalpy calculation of the quaternary is presented. According to Toop model, when constructing the quaternary geometric model, the premise is that the thermodynamics of quaternary systems shall be composed of the thermodynamics of four ternary systems, and that the interaction between ternary systems should be taken into account, regarded as the general mathematical properties of semi-empirical enthalpy of

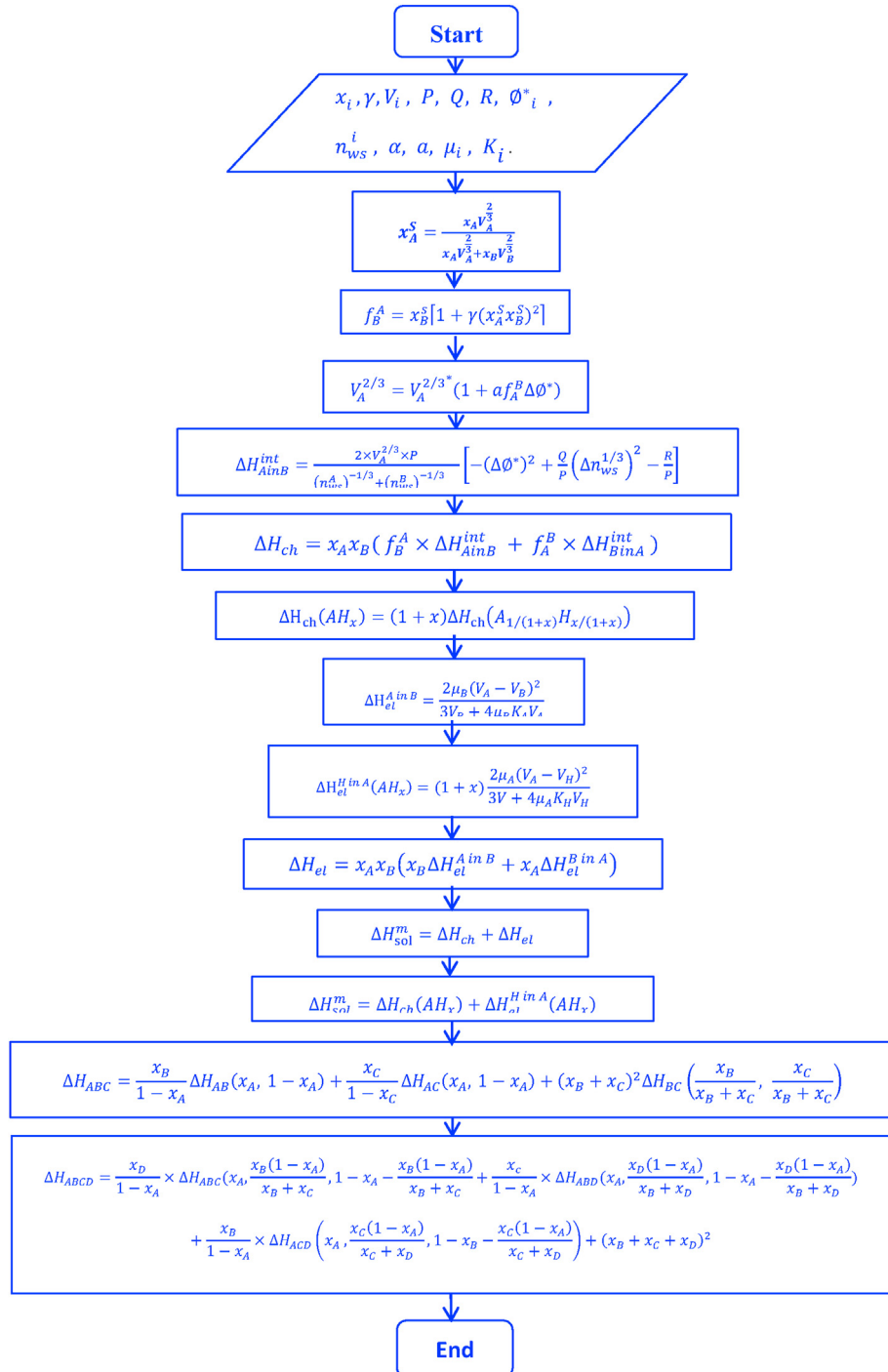


**Fig. 1 – Schematic diagram showing calculate procedure for extension of Miedema model from binary to quaternary system.**

formation models. The formation enthalpies  $\Delta H$  of quaternary alloy can be calculated as follow:

$$\begin{aligned} \Delta H_{ABCD} = & \frac{x_D}{1 - x_A} \times \Delta H_{ABC} \left( x_A, \frac{x_B(1 - x_A)}{x_B + x_C}, 1 - x_A - \frac{x_B(1 - x_A)}{x_B + x_C} \right) \\ & + \frac{x_C}{1 - x_A} \times \Delta H_{ABD} \left( x_A, \frac{x_D(1 - x_A)}{x_B + x_D}, 1 - x_A - \frac{x_D(1 - x_A)}{x_B + x_D} \right) + \frac{x_B}{1 - x_A} \\ & \times \Delta H_{ACD} \left( x_A, \frac{x_C(1 - x_A)}{x_C + x_D}, 1 - x_B - \frac{x_C(1 - x_A)}{x_C + x_D} \right) + (x_B + x_C + x_D)^2 \end{aligned}$$

$$\times \Delta H_{BCD} \left( \frac{x_B}{x_B + x_C + x_D}, \frac{x_C}{x_B + x_C + x_D}, \frac{x_D}{x_B + x_C + x_D} \right) \quad (1)$$

where  $\Delta H_{ABCD}$  stand for the formation enthalpy of quaternary alloy  $\Delta H_{ABC}$ ,  $\Delta H_{ABD}$ ,  $\Delta H_{ACD}$  and  $\Delta H_{BCD}$  for formation enthalpies of the four constituent ternaries systems. Included in Appendix are the procedures of calculating methods, thermodynamic parameters, the use of Miedema model and its

extended version for quaternary system. The specific values of parameters were listed in [Table S1](#).

## Experimental

The master  $\text{Ce}_2\text{MgNi}_2$  alloy was prepared by induction levitation melting in a water-cooled copper crucible under a helium atmosphere. The master Ce–Ni alloy was first melted thrice as a raw metal, and Mg was then adopted and melted twice for homogeneity. Appropriate amount of Mg was added to compensate for the evaporative losses of Mg during melting.

The crystal structure of the alloy was measured by Bruker-D8 Advance X-ray diffractometer (XRD) with  $\text{Cu-K}\alpha$  radiation at 45 kV and 40 mA. The Rietveld refinements were carried out using Maud soft.

The hydrogen storage properties and hydrogenation cycling of the alloys were measured by Setaram PCTPro system using the Sievert's method. About 1.0 g sample was used for hydrogen storage testing. Before the measurement, the samples were pumped at 300 °C for 4 h. Samples hydrogenation cycle consisted of absorption at 3.0 MPa for 4 h. The hydrogenation kinetic temperature was 30, 100, 150 and 200 °C, and PCT de/absorption temperature was 200, 250, 300 and 320 °C.

## Results and discussion

### Formation enthalpy of Ce–Mg–Ni–H for solid-solution

[Fig. 1](#) exhibits ternary Ce–Mg–Ni phase diagram showing the investigated compositions including their formation enthalpies. The least enthalpy value of Ce–Mg–Ni compounds is -62.0 kJ/mol and the corresponding approximate atomic ratio of Ce, Mg, Ni is 5:1:8. Theoretically,  $\text{Ce}_5\text{MgNi}_8$  can form the most stable compound. However, ternary phases in  $\text{CeMg}_2\text{Ni}_9$ ,  $\text{CeMgNi}_4$ ,  $\text{CeMg}_2\text{Ni}$ ,  $\text{Ce}_2\text{MgNi}_2$ , and  $\text{Ce}_{23}\text{Mg}_4\text{Ni}_7$  have been reported to exist commonly in the Ce–Mg–Ni ternary system. As shown in [Table 1](#), the formation enthalpies of several Ce–Mg–Ni nominal alloy compositions calculated by Miedema's model result in unstable compounds. Xie et al. [36,37] prepared Mg–5Ni–5Ce and Mg–7Ni–3Ce (wt. %) alloys. The final stable phase is metal phase (Mg), binary phase ( $\text{CeMg}_2$ ,  $\text{CeMg}_{12}$  and  $\text{Mg}_3\text{Ni}$ ) and long-period stacking ordered phase (LPSO). Lin et al. [24,38] reported the mixing enthalpy of the constituent atomic pairs in the Ce–Mg–Ni system, finding that the pronounced chemical affinity among the elements is emphasized by mechanical alloying on Mg-rich sites. Finally, the enthalpy value of the Ce–Mg–Ni is -39.0 kJ/mol, not relate with atomic ratio. [Table 1](#) shows the list of Ce–Mg–Ni ternary compounds. It can be seen that the value of our calculation of  $\text{Ce}_{14.94}\text{Mg}_{11.1}\text{Ni}_{73.96}$  is -38.9 kJ/mol, close to the given value listed. These nominal alloy compositions are decomposed into  $\text{CeMg}_2\text{Ni}_9$ ,  $\text{CeMgNi}_4$  and  $\text{CeNi}_5$  phases after fully crystallization. However, for  $\text{Ce}_{18}\text{Mg}_{80}\text{Ni}_2$  compound, Ouyang et al. [23] considered this alloy composed of  $\text{Mg}_3\text{Ce}$  phase (57 wt %),  $\text{Ce}_2\text{Mg}_{17}$  phase (29 wt %),  $\text{CeMg}$  (7 wt %),  $\text{CeMgNi}_4$  (5 wt %), and a small amount of  $\text{MgO}$  (2 wt %). Compared with others, most of the Ni exists in the ternary  $\text{CeMgNi}_4$  phase in the as-

prepared  $\text{Mg}_{80}\text{Ce}_{18}\text{Ni}_2$  alloy, and Mg phase is no longer observed. To ensure a wider Ce–Mg–Ni phase diagram, Wu et al. [39] selected ten samples by thermodynamic calculation coupled with experimental verification. With annealing at 673 K for 120 days, the selected nominal alloy compositions samples were found to contain ternary  $\text{CeMg}_2\text{Ni}_9$ ,  $\text{CeMgNi}_4$ ,  $\text{CeMg}_2\text{Ni}$ ,  $\text{Ce}_2\text{MgNi}_2$  and  $\text{Ce}_{23}\text{Mg}_4\text{Ni}_7$ . It should be reminded that the  $\text{Ce}_2\text{MgNi}_2$  and  $\text{CeNi}_5$  were obtained after annealing of the  $\text{Ce}_{35.17}\text{Mg}_{7.54}\text{Ni}_{57.29}$ . The enthalpy value obtained by Miedema's model was -62.0 kJ/mol. For single phase  $\text{Ce}_2\text{MgNi}_2$  (P), the enthalpy value of our calculation is -44.1 kJ/mol. Therefore, it is believed that  $\text{Ce}_2\text{MgNi}_2$  has a relatively negative formation enthalpy, and it is the most easily formed compound among the ternary Ce–Mg–Ni alloys.

[Table 2](#) lists the parts of formation enthalpies of several Ce/Mg/Ni hydrides based on experiments and calculations. According to our calculation of formation enthalpies of pure metal hydrides and binary hydrides, these hydrides are similar to those available in literatures. For Ce–H system, common hydrides containing  $\text{CeH}_2$  and  $\text{CeH}_3$  [40] are attributed to valence of Ce element. In the case of ignoring the effects of temperature, the equilibrium pressure of the  $\text{H}_2$  surrounding Ce is a significant thermodynamic variable along with the lowest isotherm data available in the literature for a stable  $\text{CeH}_2$ . With the increase of hydrogen pressure,  $\text{CeH}_2$  further combines with H to form more stable  $\text{CeH}_3$ . Hence, the least enthalpy value of -188.4 kJ/mol can be obtained at a corresponding atomic ratio of 3.35 wt % by estimation of the formation enthalpy of Ce–H and comparison with the actual 3.0 wt %. However, the formation enthalpy determined by calculated value of -146.0 kJ/mol is less accurate in terms of the experimental observations of -241.0 kJ/mol. Therefore, from the studies mentioned above, it can be concluded that the least formation enthalpy value of pure metal hydride is the most stable hydride, with a feasible corresponding hydrogen concentration value as the maximum binding degree of pure metal and hydrogen. For the combination of Ni and H, the formation enthalpy is estimated to be approximately 12.2 kJ/mol. In comparison with the experimental values of 8.4–10.6 kJ/mol, it is easy to obtain positive formation enthalpy values for Ni and H. It is generally considered that a positive enthalpy value, according to two element sets, is difficult to combine and easy to decompose. Therefore, for metal hydrogen-storage material, Ni element is considered as the non-hydrogen absorbing material. In course of the hydrogen desorption and absorption, Ni element plays an extremely important role. Extensive experimental and theoretical studies have been performed to explore thermodynamic properties Mg–H systems, Pozzo M et al. [41] adopted diffusion Monte Carlo (DMC) calculations to study the structural properties and thermodynamic parameters of magnesium hydride ( $\text{MgH}_2$ ), with the experimental value of 6.0 kJ/mol. However, the 0 K temperature assumed in the calculation is far beyond the scope of the application. As mentioned previously, the calculated value of Herbst [40] is -54.0 kJ/mol. Despite some deviation from the experimental value, the enthalpy value of Mg and H can be directly estimated in the different concentration ratio. Our extended value of calculation is -88.0 kJ/mol, being the enthalpy of the most stable hydride in Mg–H systems.

**Table 1 – The enthalpies of formation of several Ce–Mg–Ni compounds calculated by the Miedema's model.**

Nominal alloy composition	Observed phases	Our work $\Delta H_{sol}$ (kJ/mol)	Ref.
CeMg <sub>5</sub> Ni <sub>7</sub>	Mg\CeMg <sub>12</sub> \Mg <sub>2</sub> Ni\LPSO	-19.6	[36]
CeMg <sub>10</sub> Ni <sub>2</sub>	Mg\CeMg <sub>12</sub> \Mg <sub>2</sub> Ni\LPSO	-5.6	[36]
CeMg <sub>10</sub> Ni <sub>10</sub>	Mg\Ce <sub>2</sub> Mg <sub>17</sub> \Mg <sub>2</sub> Ni\LPSO	-13.6	[37]
CeMg <sub>5</sub> Ni <sub>15</sub>	Mg\Ce <sub>2</sub> Mg <sub>17</sub> \LPSO	-15.6	[37]
Ce <sub>4</sub> Mg <sub>88</sub> Ni <sub>8</sub>	Mg\Ce <sub>2</sub> Mg <sub>17</sub> \Mg <sub>2</sub> Ni	-2.0	[24]
Ce <sub>2</sub> Mg <sub>88</sub> Ni <sub>9</sub>	Rich-Mg	-2.1	[24]
Ce <sub>5</sub> Mg <sub>90</sub> Ni <sub>5</sub>	Mg\Ce <sub>2</sub> Mg <sub>17</sub> \Mg <sub>2</sub> Ni\Mg <sub>6</sub> Ni	-1.2	[24]
Ce <sub>5</sub> Mg <sub>91</sub> Ni <sub>4</sub>	Mg\Ce <sub>2</sub> Mg <sub>17</sub> \Mg <sub>2</sub> Ni	-1.1	[24]
Ce <sub>4</sub> Mg <sub>92</sub> Ni <sub>4</sub>	Mg\Ce <sub>2</sub> Mg <sub>17</sub> \Mg <sub>2</sub> Ni	-0.8	[24]
Ce <sub>3</sub> Mg <sub>94</sub> Ni <sub>3</sub>	Rich-Mg	-0.4	[24]
Ce <sub>10</sub> Mg <sub>70</sub> Ni <sub>20</sub>	Mg\Ce <sub>2</sub> Mg <sub>17</sub> \Mg <sub>2</sub> Ni	-8.8	[38]
Ce <sub>25</sub> Mg <sub>50</sub> Ni <sub>25</sub>	Mg\Ce <sub>2</sub> Mg <sub>17</sub> \Mg <sub>2</sub> Ni	-19.7	[38]
Ce <sub>20</sub> Mg <sub>60</sub> Ni <sub>20</sub>	Mg\Ce <sub>2</sub> Mg <sub>17</sub> \Mg <sub>2</sub> Ni	-13.1	[38]
Ce <sub>10</sub> Mg <sub>60</sub> Ni <sub>30</sub>	Mg\Ce <sub>2</sub> Mg <sub>17</sub> \Mg <sub>2</sub> Ni	-13.9	[38]
Ce <sub>13.3</sub> Mg <sub>60</sub> Ni <sub>26.7</sub>	Mg\Ce <sub>2</sub> Mg <sub>17</sub> \Mg <sub>2</sub> Ni	-14.6	[38]
Ce <sub>15</sub> Mg <sub>70</sub> Ni <sub>15</sub>	Mg\Ce <sub>2</sub> Mg <sub>17</sub> \Mg <sub>2</sub> Ni	-7.7	[38]
Ce <sub>10</sub> Mg <sub>80</sub> Ni <sub>10</sub>	Mg\Ce <sub>2</sub> Mg <sub>17</sub> \Mg <sub>2</sub> Ni	-3.7	[38]
Ce <sub>18</sub> Mg <sub>80</sub> Ni <sub>2</sub>	CeMg <sub>3</sub> \Ce <sub>2</sub> Mg <sub>17</sub> \CeMg\CeMgNi <sub>4</sub>	-2.1	[23]
Ce <sub>2.92</sub> Mg <sub>91.84</sub> Ni <sub>5.24</sub>	Mg\Mg <sub>2</sub> Ni\CeMg <sub>12</sub>	-1.1	[39]
Ce <sub>2.93</sub> Mg <sub>88.90</sub> Ni <sub>8.18</sub>	Mg\Mg <sub>2</sub> Ni\CeMg <sub>12</sub>	-1.9	[39]
Ce <sub>6.87</sub> Mg <sub>69.95</sub> Ni <sub>23.18</sub>	CeMgNi <sub>4</sub> \Ce <sub>2</sub> Mg <sub>17</sub> \Mg <sub>2</sub> Ni	-8.4	[39]
Ce <sub>15.16</sub> Mg <sub>14.9</sub> Ni <sub>69.94</sub>	CeMg <sub>2</sub> Ni <sub>9</sub> \CeMgNi <sub>4</sub>	-38.4	[39]
Ce <sub>14.94</sub> Mg <sub>11.1</sub> Ni <sub>73.96</sub>	CeMg <sub>2</sub> Ni <sub>9</sub> \CeMgNi <sub>4</sub> \CeNi <sub>5</sub>	-38.9	[39]
Ce <sub>35.17</sub> Mg <sub>7.54</sub> Ni <sub>57.29</sub>	Ce <sub>2</sub> MgNi <sub>2</sub> \CeNi <sub>2</sub>	-62.0	[39]
Ce <sub>59.13</sub> Mg <sub>27.45</sub> Ni <sub>13.42</sub>	CeNi\Ce <sub>2</sub> Ni <sub>3</sub> \Ce <sub>2</sub> MgNi <sub>2</sub>	-22.3	[39]
Ce <sub>53.65</sub> Mg <sub>8.06</sub> Ni <sub>38.29</sub>	Ce <sub>23</sub> Mg <sub>4</sub> Ni <sub>2</sub> \CeMg\Ce <sub>2</sub> MgNi <sub>2</sub>	-47.3	[39]
Ce <sub>38.78</sub> Mg <sub>50.82</sub> Ni <sub>10.4</sub>	CeMg <sub>3</sub> \CeMg\Ce <sub>2</sub> MgNi <sub>2</sub>	-13.4	[39]
Ce <sub>22.16</sub> Mg <sub>43.25</sub> Ni <sub>34.59</sub>	CeMg <sub>3</sub> \CeMgNi <sub>4</sub> \Ce <sub>2</sub> MgNi <sub>2</sub>	-27.0	[39]
CeMg <sub>2</sub> Ni <sub>9</sub> (P)	CeMg <sub>2</sub> Ni <sub>9</sub> \CeNi <sub>5</sub> \MgNi <sub>2</sub>	-23.2	[29,30]
CeMg <sub>2</sub> Ni <sub>4</sub> (P)	CeMgNi <sub>4</sub>	-40.6	[29,30]
CeMg <sub>2</sub> Ni (P)	CeMg <sub>2</sub> Ni\CeMg <sub>3</sub>	-19.7	[33]
Ce <sub>2</sub> MgNi <sub>2</sub> (P)	Ce <sub>2</sub> MgNi <sub>2</sub> \CeNi <sub>3</sub> \CeMg <sub>3</sub>	-44.2	[31,34]
Ce <sub>23</sub> Mg <sub>4</sub> Ni <sub>7</sub> (P)	Ce <sub>23</sub> Mg <sub>4</sub> Ni <sub>7</sub>	-28.5	[35]

Note: “-” data not found in the literature; “P” represents single phase.

**Table 2 – The enthalpies of formation of several Ce/Mg/Ni hydrides calculated by the Miedema's model.**

Hydride	Observed phases	Ex $\Delta H_{sol}$ (kJ/mol)	Cal $\Delta H_{sol}$ (kJ/mol)	Our work		Ref.
				$\Delta H_{sol}$ (kJ/mol)	H-storage (at. %)	
Mg–H	MgH <sub>2</sub>	-76.8	-82.0/-54.0	-88.0	2.75	[40,41,46]
Ce–H	CeH <sub>2</sub> , CeH <sub>3</sub>	-206.0, -241.0	-188.0, -146.0	-170.4, -188.4	2.00/3.35	[40,46]
Ni–H	NiH	8.410.6	5.2	12.2	0.08	[40,46]
Ce <sub>2</sub> Mg <sub>17</sub> –H	CeH <sub>x</sub> , MgH <sub>2</sub>	-61.0	-69.0/-87.0	-104.8	46.00	[38,40]
CeMg <sub>3</sub> –H	CeH <sub>2.73</sub> , MgH <sub>2</sub>	-	-87.0	-133.7	8.50	[40,42]
CeMg–H	CeH <sub>x</sub> , MgH <sub>2</sub>	-	-87.0	-166.2	4.70	[40,42]
Mg <sub>2</sub> Ni–H	Mg <sub>2</sub> NiH <sub>4</sub>	-57.9/-64.0	-64.2/-54.2/-61.5	-52.2	7.50	[4,43,44]
Mg <sub>6</sub> Ni–H	MgH <sub>2</sub> , Mg <sub>2</sub> NiH <sub>4</sub>	-	-46.0	-71.3	19.00	[24,38]
MgNi <sub>2</sub> –H	Unknown phase	-	-28.4	-16.6	6.50	[47]
CeNi <sub>5</sub> –H	CeNi <sub>5</sub> H <sub>6</sub>	-17.6	-14.0	-35.6	7.00	[40,45,48]
CeNi <sub>3</sub> –H	Unknown phase	-44.0	-32.0	-58.5	6.00	[40,45,48]

Note: “-” data not found in the literature.

The common Ce–Mg hydrides, including Ce<sub>2</sub>Mg<sub>17</sub>–H, CeMg<sub>3</sub>–H and CeMg–H, are also showed in Table 2, with the hydride phase CeH<sub>x</sub> and MgH<sub>2</sub> as final stable phase. Lin et al. [38] and Kohlmann et al. [42] investigated the component of the Ce–Mg phase, with the enthalpy value of -87.0 kJ/mol for

Ce–Mg–H, not related with atomic ratio. Hence, in our research, the formation enthalpy of all the hydrides are calculated based on the Miedema model, obtaining the corresponding maximum H-storage (at. %). In the Mg–Ni–H ternary system, the Mg<sub>2</sub>NiH<sub>4</sub> is a common intermetallic of

**Table 3 – The enthalpies of formation of several Ce–Mg–Ni–H hydrides calculated by the Miedema's model.**

Hydride	Observed phases	Theoretical H-storage $x_{\text{expt}}$ (wt. %)	$\Delta H_{\text{sol}}$ (kJ/mol)	Our work H-storage $x_{\text{calc}}$ (wt. %)	$\delta_{x_{\text{H}}}$ (%)	Ref.
CeMg <sub>5</sub> Ni <sub>7</sub> –H	MgH <sub>2</sub> , CeH <sub>2.73</sub> , Mg <sub>2</sub> NiH <sub>4</sub>	<7.00	-31.3	1.48	-	[36]
CeMg <sub>10</sub> Ni <sub>2</sub> –H	MgH <sub>2</sub> , CeH <sub>2.73</sub> , Mg <sub>2</sub> NiH <sub>4</sub>	<7.00	-17.3	3.50	-	[36]
CeMg <sub>10</sub> Ni <sub>10</sub> –H	MgH <sub>2</sub> , CeH <sub>2.73</sub> , Mg <sub>2</sub> NiH <sub>4</sub>	<5.50	-19.6	1.74	-	[37]
CeMg <sub>5</sub> Ni <sub>15</sub> –H	MgH <sub>2</sub> , CeH <sub>2.73</sub> , Mg <sub>2</sub> NiH <sub>4</sub>	<5.50	-15.0	1.79	-	[37]
Ce <sub>4</sub> Mg <sub>88</sub> Ni <sub>8</sub> –H	MgH <sub>2</sub> , CeH <sub>2.73</sub> , Mg <sub>2</sub> NiH <sub>4</sub>	-	-7.6	4.26	-	[24]
Ce <sub>3</sub> Mg <sub>88</sub> Ni <sub>9</sub> –H	MgH <sub>2</sub>	-	-6.2	3.92	-	[24]
Ce <sub>5</sub> Mg <sub>90</sub> Ni <sub>5</sub> –H	MgH <sub>2</sub> , CeH <sub>2.73</sub> , Mg <sub>2</sub> NiH <sub>4</sub>	5.30	-8.4	4.54	14.3	[24]
Ce <sub>5</sub> Mg <sub>91</sub> Ni <sub>4</sub> –H	MgH <sub>2</sub> , CeH <sub>2.73</sub> , Mg <sub>2</sub> NiH <sub>4</sub>	-	-8.1	4.73	-	[24]
Ce <sub>4</sub> Mg <sub>92</sub> Ni <sub>4</sub> –H	MgH <sub>2</sub> , CeH <sub>2.73</sub> , Mg <sub>2</sub> NiH <sub>4</sub>	-	-6.4	4.90	-	[24]
Ce <sub>3</sub> Mg <sub>94</sub> Ni <sub>3</sub> –H	MgH <sub>2</sub>	-	-4.5	5.14	-	[24]
Ce <sub>10</sub> Mg <sub>70</sub> Ni <sub>20</sub> –H	MgH <sub>2</sub> , CeH <sub>2.73</sub> , Mg <sub>2</sub> NiH <sub>4</sub>	3.90	-24.1	3.19	18.2	[38]
Ce <sub>25</sub> Mg <sub>50</sub> Ni <sub>25</sub> –H	MgH <sub>2</sub> , CeH <sub>2.73</sub> , Mg <sub>2</sub> NiH <sub>4</sub>	2.70	-62.2	2.77	2.5	[38]
Ce <sub>20</sub> Mg <sub>60</sub> Ni <sub>20</sub> –H	MgH <sub>2</sub> , CeH <sub>2.73</sub> , Mg <sub>2</sub> NiH <sub>4</sub>	3.20	-47.0	2.71	15.3	[38]
Ce <sub>10</sub> Mg <sub>60</sub> Ni <sub>30</sub> –H	MgH <sub>2</sub> , CeH <sub>2.73</sub> , Mg <sub>2</sub> NiH <sub>4</sub>	3.18	-28.6	2.55	19.8	[38]
Ce <sub>13.3</sub> Mg <sub>60</sub> Ni <sub>26.7</sub> –H	MgH <sub>2</sub> , CeH <sub>2.73</sub> , Mg <sub>2</sub> NiH <sub>4</sub>	3.18	-35.2	2.58	18.9	[38]
Ce <sub>15</sub> Mg <sub>70</sub> Ni <sub>15</sub> –H	MgH <sub>2</sub> , CeH <sub>2.73</sub> , Mg <sub>2</sub> NiH <sub>4</sub>	3.84	-32.8	3.53	8.1	[38]
Ce <sub>10</sub> Mg <sub>80</sub> Ni <sub>10</sub> –H	MgH <sub>2</sub> , CeH <sub>2.73</sub> , Mg <sub>2</sub> NiH <sub>4</sub>	4.75	-19.7	3.94	17.0	[38]
Ce <sub>18</sub> Mg <sub>80</sub> Ni <sub>2</sub> –H	CeH <sub>2.73</sub> , MgH <sub>2</sub>	4.03	-32.4	4.41	8.6	[23]
Ce <sub>2.92</sub> Mg <sub>91.84</sub> Ni <sub>5.24</sub> –H	MgH <sub>2</sub> , CeH <sub>2.51</sub> , Mg <sub>2</sub> NiH <sub>4</sub>	5.31	-24.7	4.57	13.9	[39]
Ce <sub>2.93</sub> Mg <sub>88.90</sub> Ni <sub>8.18</sub> –H	Unknown phase	-	-9.0	3.97	-	[39]
Ce <sub>6.87</sub> Mg <sub>69.95</sub> Ni <sub>23.18</sub> –H	Unknown phase	-	-44.7	3.04	-	[39]
Ce <sub>15.16</sub> Mg <sub>14.9</sub> Ni <sub>69.94</sub> –H	Unknown phase	-	-63.7	1.21	-	[39]
Ce <sub>14.94</sub> Mg <sub>11.1</sub> Ni <sub>73.96</sub> –H	Unknown phase	-	-69.2	1.34	-	[39]
Ce <sub>35.17</sub> Mg <sub>7.54</sub> Ni <sub>57.29</sub> –H	Unknown phase	-	-54.0	1.70	-	[39]
Ce <sub>59.13</sub> Mg <sub>27.45</sub> Ni <sub>13.42</sub> –H	Unknown phase	-	-74.2	2.72	-	[39]
Ce <sub>53.65</sub> Mg <sub>8.06</sub> Ni <sub>38.29</sub> –H	Unknown phase	-	-63.9	2.18	-	[39]
Ce <sub>38.78</sub> Mg <sub>50.82</sub> Ni <sub>10.4</sub> –H	Unknown phase	-	-53.8	3.22	-	[39]
Ce <sub>22.16</sub> Mg <sub>43.25</sub> Ni <sub>34.59</sub> –H	Unknown phase	-	-37.7	2.39	-	[39]
CeMg <sub>2</sub> Ni <sub>9</sub> (P)–H	Unknown phase	-	-38.3	0.97	-	[29,30]
CeMgNi <sub>4</sub> (P)–H	CeH <sub>2.52</sub> , CeMgNi <sub>4</sub> H <sub>4</sub>	-	-48.9	1.00	-	[31,32]
CeMg <sub>2</sub> Ni (P)–H	MgH <sub>2</sub> , CeH <sub>2.74</sub> , Mg <sub>2</sub> NiH <sub>4</sub>	-	-32.7	2.58	-	[33]
Ce <sub>2</sub> MgNi <sub>2</sub> (P)–H	Unknown phase	-	-59.1	1.64	-	[31,34]
Ce <sub>23</sub> Mg <sub>4</sub> Ni <sub>7</sub> (P)–H	Unknown phase	-	-77.8	2.24	-	[35]

Note: “-” data not found in the literature; “P” represents single phase.

alloy hydrides. However, as previously stated, Liang et al. [43] concluded that formation enthalpy value of ball-milled amorphous Mg<sub>2</sub>Ni hydride at high temperatures is -59.2 kJ/mol, and maximum possible hydrogen capacity is 4.5 wt%. Wang et al. [44] synthesized an intermetallic Mg<sub>2</sub>Ni alloy made by dry milling for 40 h with the hydrogen capability of approximately 4.9 wt%. Therefore, theoretically, the maximum binding degree of hydrogen can reach 6.6 wt % (7.5 at. %) when the ratio of Mg and Ni is 2:1 based on the Miedema model. This value is also correlated with the formation enthalpy value of the previous MgH<sub>2</sub> calculation. Similarly, with common Ce–Ni hydrides, including CeNi<sub>5</sub>–H and CeNi<sub>3</sub>–H, Klyamkin et al. [45] determined that the hydrogen storage capacity of CeNi<sub>5</sub> could reach 6.8 at. %, basically similar to the predicted value of 7.0 at. %. For formation enthalpy value estimation determined by pressure–composition isotherm (PCI), the value of Klyamkin is -14.6 kJ/mol on the first trial and -17.0 kJ/mol on the third trial. It is then deduced that in the ideally, the value of LaNi<sub>5</sub> can be determined to be -19.0 kJ/mol for the first time. So our deduction is that, ideally, the hydrogen storage of CeNi<sub>5</sub> is higher and the enthalpy value might be close to -33.1 kJ/mol,

the value of LaNi<sub>5</sub>. This is roughly equivalent to -35.6 kJ/mol, the estimated value of CeNi<sub>3</sub>.

**Table 3** lists the parts of formation enthalpies of several Ce–Mg–Ni–H hydrides calculated by the Miedema's model. The final stable phase is hydride phase CeH<sub>2.73</sub>, MgH<sub>2</sub>, Mg<sub>2</sub>NiH<sub>4</sub>, CeH<sub>2.52</sub>, CeMgNi<sub>4</sub>H<sub>4</sub> and CeH<sub>2.74</sub>. Thus, Lin et al. [38] obtained the theoretical capacity of the crystalline Mg–Ce–Ni alloys through calculation based on the formation of CeH<sub>2.73</sub>, MgH<sub>2</sub> and Mg<sub>2</sub>NiH<sub>4</sub>. Additionally, they provided the mixing enthalpy of the constituent atomic pairs in the Ce–Mg–Ni–H system, with the pronounced chemical affinity among the elements is emphasized by mechanical alloying on Mg-rich sites. Ultimately, the enthalpy value of the Ce–Mg–Ni–H is -142.0 kJ/mol, not correlated with atomic ratio. However, the enthalpy value of Ce<sub>53.65</sub>Mg<sub>8.06</sub>Ni<sub>38.29</sub>–H by Miedema's model is -63.9 kJ/mol. For single phase Ce<sub>2</sub>MgNi<sub>2</sub> (P)–H and Ce<sub>23</sub>Mg<sub>4</sub>Ni<sub>7</sub> (P)–H, the enthalpy values of our calculation are -59.1 and -77.8 kJ/mol, respectively. Therefore, it can be concluded that the aforementioned article mentioned that the least formation enthalpy value of hydride is also the most stable hydride, with the corresponding hydrogen concentration value as the maximum binding degree of compound and hydrogen.

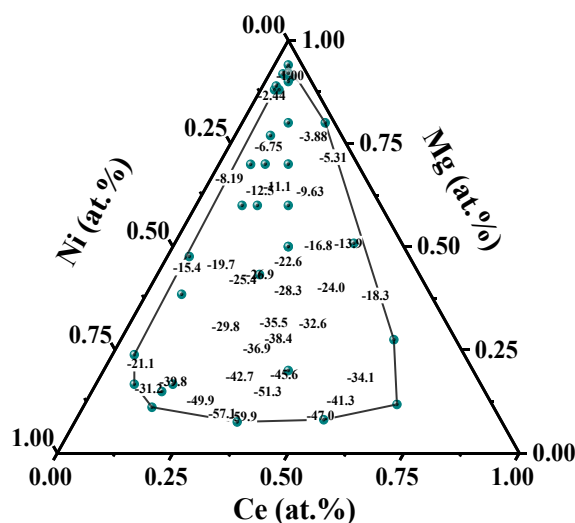


**Fig. 2 – Ternary Ce–Mg–Ni phase diagram showing the compositions investigated including the enthalpies of formation (kJ/mol).**

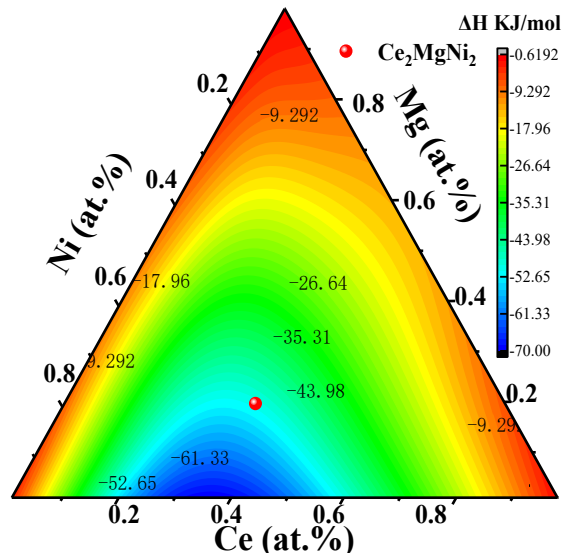


**Fig. 3 – Contour map of solid-solution state Ce–Mg–Ni mixed enthalpy.**

Notably, Xie et al. [36,37] obtained the theoretical H-storage of Mg–5Ni–5Ce and Mg–7Ni–3Ce (wt. %) alloys based on the preparing Nanocrystalline/amorphous composites by ball-milling. Ouyang et al. [23] and Wu et al. [39] selected  $\text{Ce}_{18}\text{-Mg}_{80}\text{Ni}_2\text{-H}$  and  $\text{Ce}_{2.92}\text{Mg}_{91.84}\text{Ni}_{5.24}\text{-H}$ , and determined theoretical value of H-storage to be 4.03 and 5.31 wt %, respectively. Compared with the estimated values of 4.41 and 4.57 wt % in this paper, the differences are so minimal enough to reflect the effectiveness of our work. Hence, calculations are conducted on the formation enthalpies of all the hydrides provided based on the Miedema model and obtained the corresponding maximum theoretical value of H-storage (at. %). In this paper, for maximum theoretical H-storage (at. %), the deviations of estimates are expressed as  $\delta_{x_H}$ , which is given as  $\delta_{x_H} = |x_{\text{expt}} - x_{\text{calc}}| / N$  by Herbst [46], where N is the sum of the measurements of each element including H. It is necessary to state that the error calculation in this paper is calculated in accordance with the atomic percentage  $x_{H,\text{sol}}$  (at. %) when the concentration of the alloy hydride is the atomic percentage. Compared with the experiment values found in literatures, the deviations of the estimation  $\delta_{x_H}$ , is approximately 15%.

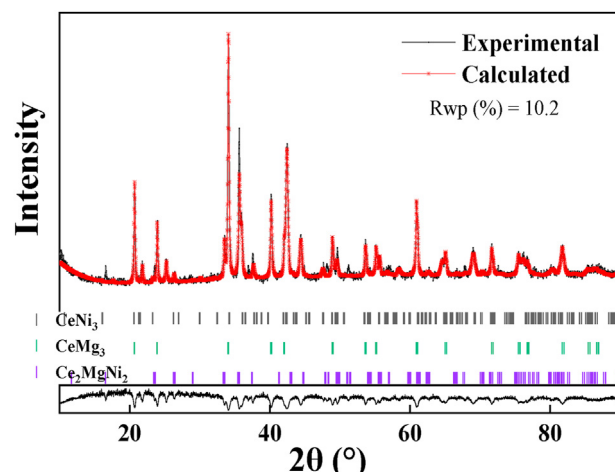
#### Formation enthalpy of $\text{Ce}_2\text{MgNi}_2$

Fig. 3 demonstrates the contour map of solid-solution state Ce–Mg–Ni mixed enthalpy, with the enthalpy of the ternary system changing with the atomic percentage concentration. In the selection of concentration, as shown in Fig. 3, x is the atomic percentage concentration, considered within the scope of  $0.1 \leq x \leq 0.9$ . The contour maps are intuitively reflected, along with the Ce, Mg and Ni constituents, and the variation tendency of the formation enthalpies caused by the composition variation of the ternary alloy. Additionally, the most negative enthalpy value range is in blue areas. Similar to

Fig. 2 and Table 2, the enthalpy value of Ce–Mg–Ni compounds is  $-62.0$  kJ/mol, and the corresponding atomic ratio of Ce, Mg, and Ni is 5:1:8. However, it is common that ternary phases of  $\text{CeMg}_2\text{Ni}_3$ ,  $\text{CeMgNi}_4$ ,  $\text{CeMg}_2\text{Ni}$ ,  $\text{Ce}_2\text{MgNi}_2$  and  $\text{Ce}_{23}\text{-Mg}_4\text{Ni}_7$  have been reported in Ce–Mg–Ni ternary system. The prepared  $\text{Ce}_2\text{MgNi}_2$  alloy is well edge in blue areas, with the range for optimized stoichiometry alloys in the contour map of the solid-solution state enthalpy. The  $\text{Ce}_2\text{MgNi}_2$  alloy is designed to investigate its hydrogen storage properties.

#### Microstructure

The XRD patterns and Rietveld analysis of the as-cast  $\text{Ce}_2\text{-MgNi}_2$  alloy are displayed in Fig. 4 with their crystallographic data summarized in Table 4, and the main phase was identified as  $\text{Ce}_2\text{MgNi}_2$ . In addition,  $\text{CeMg}_3$  and  $\text{CeNi}_3$  are observed as



**Fig. 4 – XRD and the Rietveld refinement of the as-cast  $\text{Ce}_2\text{MgNi}_2$  alloy.**

**Table 4 – Structural parameters and phase abundance of the as-cast Ce<sub>2</sub>MgNi<sub>2</sub> alloy.**

Phase structure	Abundance (wt %)	Structure type	C. S.	S. G.	a(Å)	c(Å)	$\alpha/^\circ$	$\beta/^\circ$	$\gamma/^\circ$
Ce <sub>2</sub> MgNi <sub>2</sub>	56.41	U <sub>3</sub> Si <sub>2</sub>	Tetragonal	P4/mmb	7.596	3.7671	90.00	90.00	90.00
CeMg <sub>3</sub>	22.33	BiF <sub>3</sub>	Cubic	Fm-3m	7.448	7.448	90.00	90.00	90.00
CeNi <sub>3</sub>	14.25	CeNi <sub>3</sub>	Hexagonal	P63/mmc	4.980	16.540	90.00	90.00	120.00

minor secondary phases. The presence of Ce<sub>2</sub>MgNi<sub>2</sub> alloy has a relatively negative formation enthalpy and is probably the most easily formed compound among the ternary Ce–Mg–Ni alloys. The structural parameters and phase abundance are refined and recalculated by Rietveld method using Maud program. The calculated profile is in good accordance with the measured pattern also shown in Fig. 4 with the detailed data is listed in Table 4.

### Hydrogen storage performances

To obtain the intrinsic sorption behavior, activation process was carried out preferentially through three successive sorption cycles at 200 °C (3.0 MPa hydrogen pressure for absorption). As displayed in Fig. 5, the sorption behaviors of activated as-cast Ce<sub>2</sub>MgNi<sub>2</sub> sample at 30, 100, 150 and 200 °C. From the absorption curves under 3.0 MPa hydrogen pressure in Fig. 5, it is seen that the hydrogen uptake capacity at 200 °C reaches 1.29 wt % H<sub>2</sub> in 90 min, while it takes 150 min for sorption capacity to rise up to 1.20 wt % H<sub>2</sub> at 100 and 150 °C, since the stated temperatures provide the dynamic conditions for hydrogen diffusion. It is worth mentioning that the absorption capacity of the as-cast Ce<sub>2</sub>MgNi<sub>2</sub> alloy at room temperature is 0.9 wt % H<sub>2</sub>%.

Fig. 6a) shows the PCT desorption/absorption curves of as-cast Ce<sub>2</sub>MgNi<sub>2</sub> alloy measured at 200 °C, 250 °C, 300 °C and 320 °C. The maximum hydrogen capacity reaches 1.57 wt % H<sub>2</sub> at 320 °C. Moreover, under each temperature, the absorption and desorption plateaus are all extremely flat, so the hydride formation enthalpy,  $\Delta H$ , and entropy,  $\Delta S$ , were calculated by Van't Hoff equation [49]. The Van't Hoff curves are illustrated in Fig. 6b), with the

hydrogenation enthalpy of -63.7 kJ/mol H<sub>2</sub> of the as-cast Ce<sub>2</sub>MgNi<sub>2</sub>-H. Fortunately, by Miedema's model, the enthalpy value of Ce<sub>2</sub>MgNi<sub>2</sub>-H is -59.1 kJ/mol H<sub>2</sub>. Thus, it can be seen that the enthalpy value of Ce<sub>2</sub>MgNi<sub>2</sub>-H in keeping with the hydride formation enthalpy of as-cast Ce<sub>2</sub>MgNi<sub>2</sub>-H could be obtained by Van't Hoff equation. Moreover, the maximum hydrogen capacity of as-cast Ce<sub>2</sub>MgNi<sub>2</sub> alloy is 1.57 wt % H<sub>2</sub> determined by PCT curves at 320 °C. The maximum hydrogen capacity is also consistent with theoretical H-storage 1.64 wt % H<sub>2</sub>. Thus, the modeling enthalpies data are made almost identical to experimental results. Additionally, hydrogenation entropy of Ce<sub>2</sub>MgNi<sub>2</sub> alloy for hydrogen absorption is -102.8 J/mol K H<sub>2</sub>. The desorption enthalpy of Ce<sub>2</sub>MgNi<sub>2</sub>-H is 78.4 kJ/mol H<sub>2</sub>, and desorption entropy is 127.7 J/mol K H<sub>2</sub>.

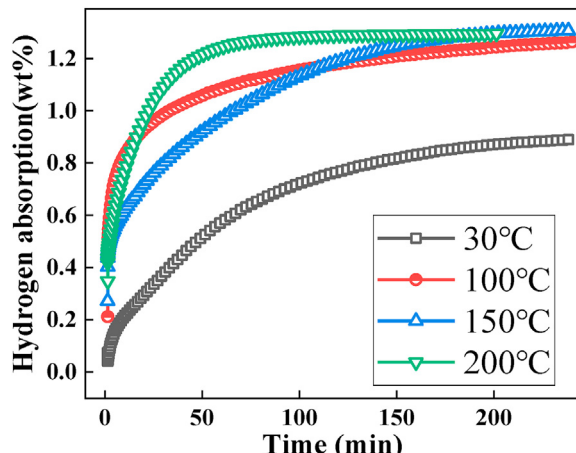


Fig. 5 – Isothermal hydrogenation kinetic curves of as-cast Ce<sub>2</sub>MgNi<sub>2</sub> alloy at different temperatures.

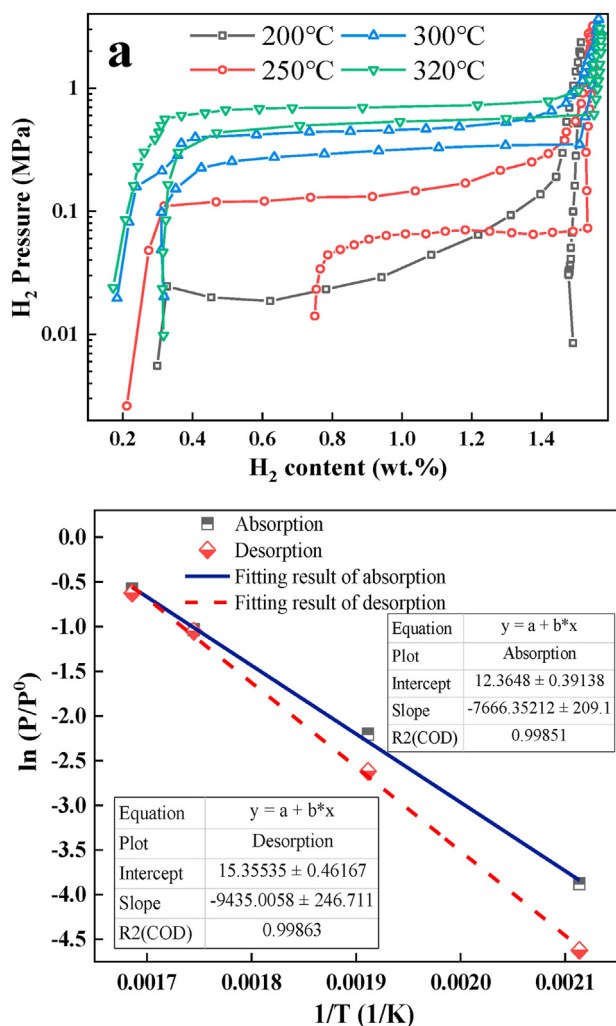


Fig. 6 – a) PCT de/absorption curves of as-cast Ce<sub>2</sub>MgNi<sub>2</sub> alloy at different temperature; b) Van't Hoff curves.

## Conclusions

An extended semi-empirical model has been developed for estimating the hydrogen content and formation enthalpy of Ce–Mg–Ni–H, and further deduced to a methodology for predicting the maximum hydrogen capacity of the hydrides. By comparing the calculation results, the following conclusions can be drawn:

- 1) The enthalpies of the ternary hydrides Ce–Mg–Ni–H coincided with the trends of the experimental data. This further clarified that the extended Miedema's model is feasible in estimating the enthalpies of these systems.
- 2) The formation enthalpy of Ce<sub>2</sub>MgNi<sub>2</sub>–H<sub>2</sub> could be calculated by the extended Miedema theory, with the least enthalpy value of –59.1 kJ/mol H<sub>2</sub> corresponding to the hydrogen content of 1.64 wt % H<sub>2</sub>.
- 3) The as-cast Ce<sub>2</sub>MgNi<sub>2</sub> alloy was prepared. The reaction enthalpy is –63.7 kJ/mol H<sub>2</sub> obtained by Van't Hoff equation. The maximum hydrogen capacity reaches 1.57 wt % H<sub>2</sub>.
- 4) The enthalpy value of Ce<sub>2</sub>MgNi<sub>2</sub>–H was calculated by Miedema's model and it keeps with the hydride formation enthalpy of as-cast Ce<sub>2</sub>MgNi<sub>2</sub>–H obtained by Van't Hoff equation.

## Declaration of competing interest

The authors declare that they have no known competing financial interests or personal relationships that could have appeared to influence the work reported in this paper.

## Acknowledgements

This work was supported by the National Natural Foundations of China (No. 51871125, 51962028, 51961032), Application Technology Research and Development Foundation of Inner Mongolia, China (No. 2019MS05056, 2018MS05040).

## Appendix A. Supplementary data

Supplementary data to this article can be found online at <https://doi.org/10.1016/j.ijhydene.2020.10.195>.

## REFERENCES

- [1] Wilmer CE, Leaf M, Lee CY, Farha OK, Hauser BG, Hupp JT, Snurr RQ. Large-scale screening of hypothetical metal–organic frameworks. *Nat Chem* 2011;4:83–9.
- [2] Pulido A, Chen L, Kaczorowski T, Holden D, Little MA, Chong SY, Slater BJ, McMahon DP, Bonillo B, Stackhouse CJ, Stephenson A, Kane CM, Clowes R, Hasell T, Cooper AI, Day GM. Functional materials discovery using energy–structure–function maps. *Nature* 2017;543:657–64.
- [3] King DJM, Middleburgh SC, McGregor AG, Cortie MB. Predicting the formation and stability of single phase high-entropy alloys. *Acta Mater* 2016;104:172–9.
- [4] Rahnama Alireza, Zepon Guilherme, Seetharaman Sridhar. Machine learning based prediction of metal hydrides for hydrogen storage, part I: prediction of hydrogen weight percent. *Int J Hydrogen Energy* 2019;44:7345–53.
- [5] Li Q, Li Y, Liu B, Lu X, Zhang T, Gu Q. The cycling stability of the in situ formed Mg-based nanocomposite catalyzed by YH<sub>2</sub>. *J Mater Chem* 2017;5:17532–43.
- [6] Wang Q, Li J-H, Liu B-X. Thermodynamic predicting and atomistic modeling the favored compositions for Mg–Ni–Y metallic glasses. *RSC Adv* 2015;5:60220–9.
- [7] Wang Y, Do Northwood. Calculation of the enthalpy of metal hydride formation. *J Less-Common Met* 1987;135:239–49.
- [8] Bouter PCP, Miedema AR. On the heats of formation of the binary hydrides of transition metals. *J Less-Common Met* 1980;71:147–61.
- [9] D Boer FR, Boom R, M Mattens WC, Miedema AR, Niessen AK. Cohesion in metals: transition metal alloys. Amsterdam: North-Holland; 1988.
- [10] Rafiei M, Enayati MH, Karimzadeh F. Thermodynamic analysis of solid solution formation in the nanocrystalline Fe–Ti–Al ternary system during mechanical alloying. *J Chem Thermodyn* 2013;58:243–9.
- [11] Musial A, Śniadecki Z, Idzikowski B. Thermal stability and glass forming ability of amorphous Hf<sub>2</sub>Co<sub>11</sub>B alloy. *Mater Des* 2017;114:404–9.
- [12] Yakymovych A, Fürtauer S, Flandorfer H, Ipser H. Enthalpies of mixing of liquid ternary Co–Li–Sn alloys. *Inside Chem* 2014;145:1697–706.
- [13] Mourani MT, Golikand AN, Asadabad MA. Comparative thermodynamic analysis of nanocrystalline and amorphous phase formation in Nb/Al and Nb/Sn systems during mechanical alloying. *J Supercond Nov Magnetism* 2016;29:1467–74.
- [14] Mousavi MS, Abbasi R, Kashani-Bozorg SF. A thermodynamic approach to predict formation enthalpies of ternary systems based on Miedema's model. *Metall Mater Trans* 2016;47:3761–70.
- [15] Wang W, Li J, Yan H, Liu B. A thermodynamic model proposed for calculating the standard formation enthalpies of ternary alloy systems. *Scripta Mater* 2007;56:975–8.
- [16] Aguilar C, Guzman P, Lascano S, Parra C, Bejar L, Medina A, Guzman D. Solid solution and amorphous phase in Ti–Nb–Ta–Mn systems synthesized by mechanical alloying. *J Alloys Compd* 2016;670:346–55.
- [17] Sreekumar VM, Ravi KR, Pillai RM, Pai BC, Chakraborty M. Thermodynamics and kinetics of The formation of Al<sub>2</sub>O<sub>3</sub>/MgAl<sub>2</sub>O<sub>4</sub>/MgO in Al-silica metal matrix composite. *Metall Mater Trans* 2008;39:919–33.
- [18] Jacob KT, Dhiman AK, Gupta P. System Gd–Rh–O: thermodynamics and phase relations. *J Alloys Compd* 2013;546:185–91.
- [19] Wang C, Chen G, Wang X, Zhang Y, Yang W, Wu G. Effect of Mg content on the thermodynamics of interface reaction in Cf/Al composite. *Metall Mater Trans A* 2012;43:2514–9.
- [20] Fan T, Zhang C, Chen J, Zhang D. Thermodynamics and kinetics to alloying addition on in-situ AlN/Mg composites synthesis via displacement reactions in liquid Mg melt. *Metall Mater Trans* 2009;40:2743–50.
- [21] Haowen X, Bangwei Z. Effects of preparation technology on the structure and amorphous forming region for electroless Ni–P alloys. *J Mater Process Technol* 2002;124:8–13.
- [22] Matysik P, Czujko T, Varin RA. The application of Pettifor structure maps to binary metal hydrides. *Int J Hydrogen Energy* 2014;39:398–405.
- [23] Ouyang L-Z, Yang X-S, Zhu M, Liu J-W, Dong H-W, Sun D-L, Zou J, Yao X-D. Enhanced hydrogen storage kinetics and

- stability by synergistic effects of *in situ* formed CeH<sub>2.73</sub> and Ni in CeH<sub>2.73</sub>-MgH<sub>2</sub>-Ni nanocomposites. *J Phys Chem C* 2014;118:7808–20.
- [24] Lin H-J, Ouyang L-Z, Wang H, Zhao D-Q, Wang W-H, Sun D-L, Zhu M. Hydrogen storage properties of Mg-Ce-Ni nanocomposite induced from amorphous precursor with the highest Mg content. *Int J Hydrogen Energy* 2012;37:14329–35.
- [25] Shang C-X, Guo Z-X. Structural and desorption characterisations of milled (MgH<sub>2</sub>pY, Ce) powder mixtures for hydrogen storage. *Int J Hydrogen Energy* 2007;32:2920. 5.
- [26] Yong H, Guo S-H, Yuan Z-M, Qi Y, Zhao D-L, Zhang Y-H. Catalytic effect of *in situ* formed Mg<sub>2</sub>Ni and REHx (RE: Ce and Y) on thermodynamics and kinetics of Mg-RE-Ni hydrogen storage alloy. *Renew Energy* 2020;157:828–39.
- [27] Liu Z-C, Ruan F, Li Y-M, Zhai T-T, Zhao M, Zhang J-Y. Modeling of amorphous phase formation and its thermodynamic behaviour in CeMgH, CeNiH and MgNiH. *Intermetallics* 2019;105:79–91.
- [28] Wang X-L, Tu J-P, Wang C-H, Zhang X-B, Chen C-P, Zhao X-B. Hydrogen storage properties of nanocrystalline Mg-Ce/Ni composite. *J Power Sources* 2006;159:163–6.
- [29] Kadir K, Sakai T, Uehara I. Synthesis and structure determination of a new series of hydrogen storage alloys; RMg<sub>2</sub>Ni<sub>9</sub> (R=La, Ce, Pr, Nd, Sm and Gd) built from MgNi<sub>2</sub> Laves-type layers alternating with AB<sub>5</sub> layers. *J Alloys Compd* 1997;257:115–21.
- [30] Cromer DT, Olsen CE. The crystal structure of PuNi<sub>3</sub> and CeNi<sub>3</sub>. *Acta Crystallogr* 1959;12:689–94.
- [31] Geibel C, Klinger U, Weiden M, Buschinger B, Steglich F. Magnetic properties of new Ce-T-Mg compounds (T = Ni, Pd). *Physica B* 1997;s237–238:202–4.
- [32] Kadir K, Noréus D, Yamashita I. Structural determination of AMgNi<sub>4</sub> (where A=Ca, La, Ce, Pr, Nd and Y) in the AuBe<sub>5</sub> type structure. *J Alloys Compd* 2002;345:140–3.
- [33] Pei L, Han S, Wang J, Hu L, Zhao X, Liu B. Hydrogen storage properties and phase structures of RMg<sub>2</sub>Ni (R=La, Ce, Pr, Nd) alloys. *Mater Sci Eng B* 2012;177:1589–95.
- [34] Pottgen R, Fugmann A, Hoffmann RD, Rodewald UC, Niepmann D. Intermetallic cerium compounds with ordered U<sub>3</sub>Si<sub>2</sub> type structure. *Z Naturforsch* 2000;55b:155–61.
- [35] Tuncel S, Hermes W, Chevalier B, Rodewald UC, Pottgen R. Ternary magnesium compounds RE<sub>23</sub>Ni<sub>7</sub>Mg<sub>4</sub> (RE=La, Ce, Pr, Nd, Sm) with Pr<sub>23</sub>Ir<sub>7</sub>Mg<sub>4</sub> type structure. *Z Anorg Allg Chem* 2008;634:2140–4.
- [36] Xie L-S, Li J-S, Zhang T-B, Song L, Kou H-C. Microstructure and hydrogen storage properties of Mg-Ni-Ce alloys with a long-period stacking ordered phase. *J Power Sources* 2017;338:91–102.
- [37] Xie L-S, Li J-S, Zhang T-B, Song L, Kou H-C. De/hydrogenation kinetics against air exposure and microstructure evolution during hydrogen absorption/desorption of Mg-Ni-Ce alloys. *Renew Energy* 2017;113:1399–407.
- [38] Lin H-J, He M, Pan S-P, Gu L, Li H-W, Wang H, Ouyang L-Z, Liu J-W, Ge T-P, Wang D-P, Wang W-H, Akiba Etsuo, Zhu M. Towards easily tunable hydrogen storage via a hydrogen-induced glass-to-glass transition in Mg-based metallic glasses. *Acta Mater* 2016;120:68–74.
- [39] Wu K-B, Luo Q, Chen S-L, Gu Q-F, Chou K-C, Wang X-L, Li Q. Phase equilibria of Ce-Mg-Ni ternary system at 673 K and hydrogen storage properties of selected alloy. *Int J Hydrogen Energy* 2016;41(3):1725–35.
- [40] Herbst JF. On estimating the enthalpy of formation and hydrogen content of quaternary hydrides. *J Alloys Compd* 2004;368:221–8.
- [41] Pozzo M, Alfè D. Structural properties and enthalpy of formation of magnesium hydride from quantum Monte Carlo calculations. *Phys Rev B* 2008;77:77–82.
- [42] Kohlmann H. From magnesium based intermetallics to metal hydrides: structures, properties and reaction pathways. *Z Kristallogr* 2010;225:195–200.
- [43] Liang G, Boily S, Huot J, Van Neste A, Schulz R. Mechanical alloying and hydrogen absorption properties of the Mg–Ni system. *J Alloys Compd* 1998;267:302–6.
- [44] Wang H, Chyou S, Wang S, Yang M, Hsu C, Tien H, Huang N. Amorphous phase formation in intermetallic Mg<sub>2</sub>Ni alloy synthesized by ethanol wet milling. *J Alloys Compd* 2009;479:330–3.
- [45] Yakovleva NA, Klyamkin SN, Veremeeva OA, Tsikhotskaya AA. Specific features of the thermodynamics of activation in the LaNi<sub>5</sub>-H<sub>2</sub> and CeNi<sub>5</sub>-H<sub>2</sub> systems. *Russ Chem B+* 2005;1:135–40.
- [46] Herbst JF. On extending Miedema's model to predict hydrogen content in binary and ternary hydrides. *J Alloys Compd* 2002;337:99–107.
- [47] Miled A, Askri F, Ben Nasrallah S. Numerical study of the dynamic behavior of a metal hydride pump. *Int J Hydrogen Energy* 2015;40:1083–95.
- [48] Denys RV, Yartys VA, Sato M, Riabov AB, Delaplane RG. Crystal chemistry and thermodynamic properties of anisotropic Ce<sub>2</sub>Ni<sub>7</sub>H<sub>4.7</sub> hydride. *J Solid State Chem* 2007;180:2566–76.
- [49] Yong H, Guo S-H, Yuan Z-M, Qi Y, Zhao D-L, Zhang Y-H. Catalytic effect of *in situ* formed Mg<sub>2</sub>Ni and REHx (RE: Ce and Y) on thermodynamics and kinetics of Mg-RE-Ni hydrogen storage alloy. *Renew Energy* 2020;157:828–39.